

## ONE DECADE MICROWAVE FORWARD NETWORK ANALYZER BASED ON THE MULTI-PORT TECHNIQUE

K. Haddadi\* and T. Lasri

Institut d'Electronique, de Microélectronique et de Nanotechnologie (IEMN), UMR CNRS 8520, Université Lille 1, Avenue Poincaré B. P. 60069 — 59652 Villeneuve d'Ascq Cedex — France

**Abstract**—This paper presents a one decade low-cost forward network analyzer based on a modified six-port technique. An instrumentation integrating the hardware and software resources offering advantages such as robustness and compactness is developed. The microwave part of the system is fabricated in planar technology. Associated to this system, a one-step calibration procedure is implemented on an 8-bits microcontroller. The performance, in term of measurement accuracy, is evaluated by comparing the results obtained from the system proposed to those given by a conventional network analyzer in the frequency band 1–10 GHz.

### 1. INTRODUCTION

Automatic network analyzers (ANA), introduced in the 1970's, are fundamental tools to measure the electrical properties of materials and circuits in a broad frequency range [1]. However, even if these modern instruments have been successfully applied in a wide variety of applications, their complexity, sophistication and cost have limited their applications to a laboratory environment. Recently, efforts have been made to develop and commercialize compact network analyzers to facilitate their penetration in an industrial context. Despite these efforts, one can note that the solutions proposed remain oversized and expensive for industrial purposes.

One of the most promising alternatives to the complex heterodyne principle of the ANA introduced in 1972 by Engen and Hoer is the six-port reflectometer (SPR) [2]. The proposed technique relies on power

---

*Received 27 April 2012, Accepted 4 June 2012, Scheduled 11 June 2012*

\* Corresponding author: Kamel Haddadi (kamel.haddadi@iemn.univ-lille1.fr).

measurements rather than mixing products to determine the complex reflection coefficient of a device under test [3]. In comparison with the ANA topology, the six-port architecture is reduced to a passive linear circuit associated to power detectors. Since the introduction of the six-port technique, there has been considerable work in the analysis and realization of six-port reflectometers [4–8]. The six-port concept takes also advantage of the capability of easily and accurately retrieving the magnitude and phase of a complex microwave signal in different kind of applications such as radar sensors [9–12] and telecommunications [13–16].

By using two six-port reflectometers in a dual six-port configuration, C. A. Hoer has shown in 1977 the possibility to measure all of the  $S$ -parameters of any linear reciprocal or nonreciprocal, passive or active two-port network [17]. Since then, extensive works have been made to develop automated dual six-port network analyzers to compete with commercial conventional solutions [18–20]. Despite these studies, the measurement of the four-parameters of a two-port network by using the six-port technique still requires more efforts in both hardware and software resources than for the usual SPR.

From the previous considerations, the question arises on how to simultaneously extend the measurement capabilities of six-port systems and preserve the advantages of the technique (low-cost, low-power consumption, compactness, simplicity of operation). If we restrict the measurement to only the complex reflection coefficient ( $S_{11}$ ) and the complex transmission coefficient ( $S_{21}$ ) of a two-port network, the architecture and the calibration task can be drastically simplified. It has to be mentioned that several applications are concerned by this type of characterization. In particular, microwave non-destructive testing and evaluation techniques that require the measurement of reflected or/and transmitted signals through the material under investigation are among the most promising ones. Consequently, the development of microwave systems capable of measuring the reflection coefficient  $S_{11}$  and the transmission coefficient  $S_{21}$  is desirable. Consequently, in this work, a forward network analyzer based on the six-port technique is investigated. Compared to previous works related to the development of six-port network analyzers, major improvements in both hardware and software resources are discussed. First, the circuit architecture proposed is based on the use of four-port correlators instead of conventional six-port ones [21]. The four-port correlator is a passive demodulator that requires only two quadratic detectors (instead of four in six-port correlators) to determine the magnitude and phase of a complex microwave signal. Associated to the circuit, a calibration model that

expresses directly and accurately the power measurements as a function of the  $S$ -parameters is developed to take into account the imperfections brought by the fabrication of the system.

The design and analysis of the four-port forward network analyzer are given in Section 2. In Section 3, the realization and the electrical characterization are described. The comparison between practical results and those obtained by a conventional network analyzer is presented in Section 4 to demonstrate the validity of the system developed.

## 2. DESIGN AND ANALYSIS

The design of the system is based on the use of a four-port correlator (Fig. 1). This system, introduced by the authors in 2008 [21], is a passive demodulator made of four Wilkinson power dividers (WD), a  $-\pi/2$  phase-shifter and two quadratic detectors (QD).

The two coherent input signals  $a_1(t)$  and  $a_2(t)$  with respective amplitudes  $A_1$  and  $A_2$  and phase-shifts  $\Phi_1$  and  $\Phi_2$  are added under two different phase-shifts ( $\varphi_1$  and  $\varphi_2$ ). The DC voltages  $V_1$  and  $V_2$  detected by the quadratic detectors at ports 3 and 4 (Fig. 1) are given by the following expressions

$$V_1 = \frac{1}{4}A_1^2 + A_2^2 + 2A_1A_2 \cos(\Phi_1 - \Phi_2) \quad (1)$$

$$V_2 = \frac{1}{4}A_1^2 + A_2^2 + 2A_1A_2 \sin(\Phi_1 - \Phi_2). \quad (2)$$

These relations associated to a calibration procedure allow to determine the magnitude ratio  $A_2/A_1$  and the relative phase-shift  $\Phi_1 - \Phi_2$  [21].

As the four-port correlator makes use of only two quadratic detectors instead of six in conventional six-port systems, the circuit size, the complexity and the power consumption are minimized.

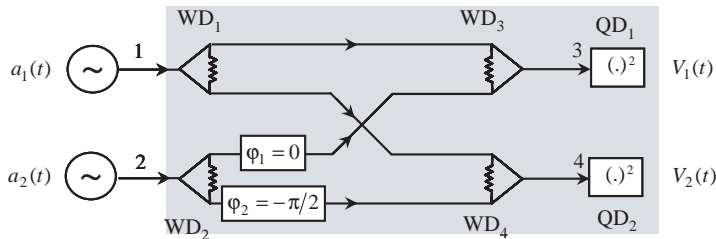


**Figure 1.** Topology of the four-port correlator.

Another advantage brought by this architecture is the use of Wilkinson power dividers instead of hybrids commonly found in six-port systems that allows to extend the frequency band capabilities. Based on this architecture, we have successfully proposed a variety of systems to address different microwave and millimetre-wave applications. Among these works, a four-port reflectometer has been demonstrated for the measurement of reflection coefficients [23]. A four-port range finder has been developed for distance measurement at 2.45 GHz [24]. A near-field microwave microscope has been developed for subsurface sensing applications [25]. A four-port receiver has been proposed for telecommunications applications [26, 27]. Altogether these studies have demonstrated that the well-known six-port system can be simplified to a four-port version without altering the measurement performances for a wide range of microwave and millimetre-wave applications.

It has to be mentioned that a preliminary study on four-port systems for network analysis has been introduced in [23]. The present study gives a complete picture of the four-port forward network analyzer including general theory, fabrication, electrical characterization, implementation of new calibration algorithms and measurement performance. The proposed architecture includes a source, three Wilkinson power dividers and two four-port correlators (Fig. 2). Two Wilkinson power dividers ( $WD_1$  and  $WD_2$ ) split the

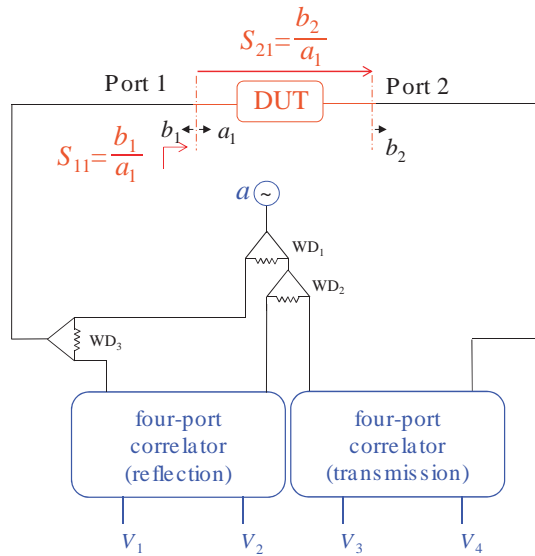


**Figure 2.** Four-port forward analyzer suitable for the measurement of the reflection ( $S_{11}$ ) and the transmission ( $S_{21}$ ) coefficients of a device under test.

source power ( $a$ ) to generate the reference signals at the input ports of the correlators. The third power divider  $WD_3$  delivers the signal to the measurement port (Port 1) and injects the reflected one to the input port of the correlator operating in reflection mode. The transmitted signal through the DUT is injected to the second port (Port 2) of the correlator operating in transmission mode. The output powers are then measured by the detectors to provide the four DC voltages  $V_1$  to  $V_4$ . From the detected voltages, the reflection and the transmission coefficients can then be retrieved by a suitable calibration procedure.

Traditional calibration algorithms do not take into account mismatching and non-linearity effects in planar six-port systems. To that end, we have recently introduced an original calibration technique based on a Spatial Fourier Analysis to take into account the imperfections brought by the fabrication of the system [22]. Furthermore, all the previous methods assume a linear response at the four arms of the six-port systems, but most of the power detection circuits are built with non-linear diodes that require an additional calibration step to linearize the diodes. In comparison with previous reported works, our calibration method includes the linearization of the power detectors as a part of the calibration procedure itself. Finally, the proposed technique gives the possibility to extend the frequency band capabilities by suitable calibration software that takes into account the hardware limitations.

In this work, the calibration model developed for six-port reflectometer is expanded to the four-port forward network analyzer proposed. The detected voltages  $V_1$  to  $V_4$  can be written as

$$V_i = x_{i0} + x_{i1} |S_{11}|^2 + \sum_2^n (x_{in} |S_{11}|^n \cos(n\Phi_{11}) + x_{i(n+1)} |S_{11}|^n \sin(n\Phi_{11}))$$

for  $i = 1, 2$  (3)

where  $\Phi_{11} = \arg(S_{11})$

$$V_i = x_{i0} + x_{i1} |S_{21}|^2 + \sum_2^n (x_{in} |S_{21}|^n \cos(n\Phi_{21}) + x_{i(n+1)} |S_{21}|^n \sin(n\Phi_{21}))$$

for  $i = 3, 4$  (4)

where  $\Phi_{21} = \arg(S_{21})$ .

In these models,  $n$  denotes the order of expansion of the Spatial Fourier analysis and  $x_{in}$  are related to real calibration coefficients determined by a two-step calibration procedure. First, an impedance tuner is connected to the port 1 whereas a matched load is connected to the port 2 (Fig. 2). The detected voltages  $V_1$  and  $V_2$  are then recorded for each position of the impedance tuner. The terms  $x_{in}$  (for  $i = 3, 4$ )

are then determined by fitting the model (3) to the measured data. In the second step, variable phase-shifter and attenuator are associated and connected between the measurement ports. The measured voltages  $V_3$  and  $V_4$  for multiple combinations of magnitude and phase-shift of the transmission coefficient  $S_{21}$  are used to determine the remaining constants  $x_{in}$  (for  $i = 3, 4$ ) by fitting the model (4) to the data recorded. The calibration procedure is straightforward and can be easily implemented on an embedded microcontroller.

After calibration, the reflection and transmission coefficients of the DUT are retrieved from the voltages measured by the detectors and an inversion procedure of the models (3) and (4). The main constraint that occurs in the resolution of the inverse problem is the non-linear nature of the equations, which are solved by numerical calculation algorithm. An initial guess of the reflection and transmission coefficients is first calculated analytically from the four voltages  $V_i$  ( $i = 1, \dots, 4$ ) values provided by the system by using a first order model (i.e., Equations (3) and (4) where  $n = 1$ ). The resolution of the Equations (3) and (4) is then achieved by using a numerical Newton-Raphson procedure. Like all the iterative procedures, the Newton-Raphson method requires a criterion to determine the convergence of the solution. For this purpose, we measure the difference between the two last computed values putting an end to the iteration when this difference is lower than the criterion precision. If the criteria precision is not satisfied, the calculated reflection and transmission coefficients are injected at the entry of the inversion process for a new iteration of the algorithm.

The realisation of the system including the microwave circuit and the microcontroller is presented in the next section.

### 3. FABRICATION AND ELECTRICAL CHARACTERIZATION

The system has been designed in planar technology and fabricated on an FR4 Epoxy substrate ( $\varepsilon = 4.8$ ). The microwave elements (Wilkinson divider, phase-shifter, quadratic detector) have been initially designed at 2.5 GHz and optimized to yield good electrical performances in the frequency band 1–4 GHz. The phase-shifters have been implemented using microstrip transmission delay lines. 100  $\Omega$  CMS resistors are used in the Wilkinson power divider topology. The detection circuit is based on an Agilent Technology HSMS-2850 zero-bias Schottky diode. The detection circuits are completed by a signal conditioning block consisting of DC operational amplifiers with an adjustable gain.

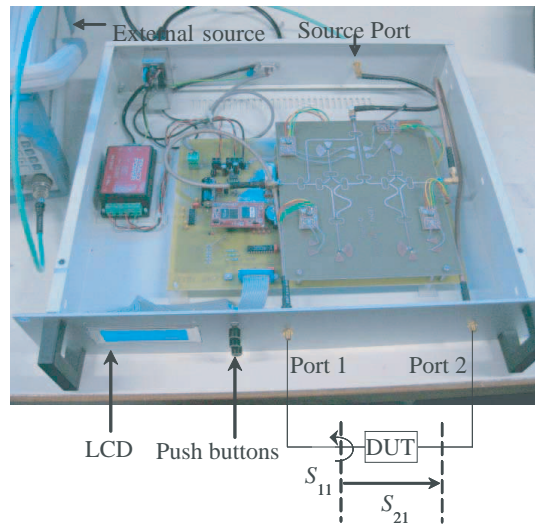


**Figure 3.** Photograph of the four-port forward network analyzer.

An electronic instrumentation has been developed to provide an easy to use facility (Fig. 3). Via three push buttons and a LCD, the system can be easily calibrated and friendly used for measurements. The calibration procedure and the inverse problem for the retrieval of the  $S$ -parameters have been implemented in an 8-bits Rabbit microcontroller. Data transfer ( $S$ -parameters, calibration constants) are done through a RS-232 link. The microwave source is external because it depends on the application aimed. Indeed, a single oscillator is sufficient for applications at a single frequency whereas a phase-locked source is needed to achieve broadband measurements. For laboratory tests, a microwave signal generator Agilent E8257C is connected to the source port.

The first test concerns the verification of the good behavior of the detectors. Two matched loads are connected to the measurement ports to make the diodes responses dependent only on the source signal. As an illustration, we present in Fig. 4 the detected voltages  $V_i$  ( $i = 1, \dots, 4$ ) after DC amplification for a source power  $P$  varying from  $-25$  to  $0$  dBm at the test frequency  $2.5$  GHz. It is noticed that the detected voltage presents a quadratic response for input source powers from about  $-25$  to  $-5$  dBm (beginning of the DC amplification stage saturation).

To characterize the functioning of the detectors in all the frequency range of interest, in the following, the quadratic areas are determined

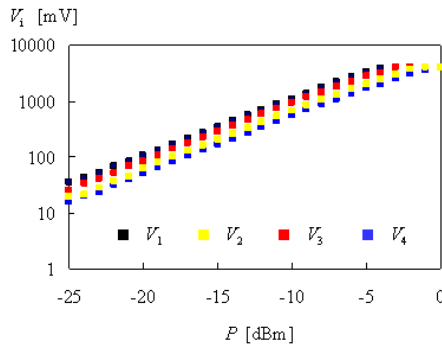


**Figure 4.** Detected voltages  $V_i$  ( $i = 1, \dots, 4$ ) after DC amplification as a function of the source power  $P - F = 2.5$  GHz.

**Table 1.** Quadratic areas of the detectors as a function of the operating frequency.

| Frequency (GHz) | Quadratic area (dBm)         |                              |                              |                              |
|-----------------|------------------------------|------------------------------|------------------------------|------------------------------|
|                 | $V_1$                        | $V_2$                        | $V_3$                        | $V_4$                        |
| 1               | $[-15,0]$                    | $[-25,0]$                    | $[-25,0]$                    | $[-25,0]$                    |
| <b>2.5</b>      | <b><math>[-25,-5]</math></b> | <b><math>[-25,-5]</math></b> | <b><math>[-25,-5]</math></b> | <b><math>[-25,-5]</math></b> |
| 4               | $[-25,-7]$                   | $[-25,-5]$                   | $[-25,-7]$                   | $[-25,-7]$                   |
| 6               | $[-12,0]$                    | $[-25,0]$                    | $[-12,0]$                    | $[-25,0]$                    |
| 8               | $[-15,0]$                    | $[-15,0]$                    | $[-15,0]$                    | $[-15,0]$                    |
| 10              | $[-12,8]$                    | $[-9.5,5.5]$                 | $[-12,8]$                    | $[-12,8]$                    |

for different test frequencies up to 10 GHz. Table 1 resumes the results obtained. For each test frequency, the input source power is varied from  $-25$  dBm to a value that corresponds to the saturation of the DC amplifiers.

These results show a good functioning of the detectors in the whole frequency band 1–10 GHz even if the microwave system has been initially designed and optimized between 1 and 4 GHz. For frequencies greater than 4 GHz, the source power must be increased to compensate the losses in the microwave circuit.

To foresee measurements up to 10 GHz, in addition to the fact that the detection circuits are quadratic in the frequency range 1–10 GHz, one has to verify if the Equations (3) and (4) are still able to model accurately the detected voltages as a function of the reflection coefficient  $S_{11}$  and the transmission coefficient  $S_{21}$  to be measured.



In the next section, measurements are provided up to 10 GHz to determine to what extent the calibration technique (software) can take into account the hardware limitations.

4. MEASUREMENT PERFORMANCE

The  $S$ -parameters of the device under test are retrieved from the voltages measured by the detectors and an inversion procedure of the models (3) and (4). As the two four-port correlators included in the system operate independently (Fig. 2), the performance of the system can be studied separately in terms of reflection or transmission coefficients measurement. For comparison purposes, the calibration constants of the models (3) and (4) have been determined at the second order ( $n = 2$ ) and the third order ( $n = 3$ ).

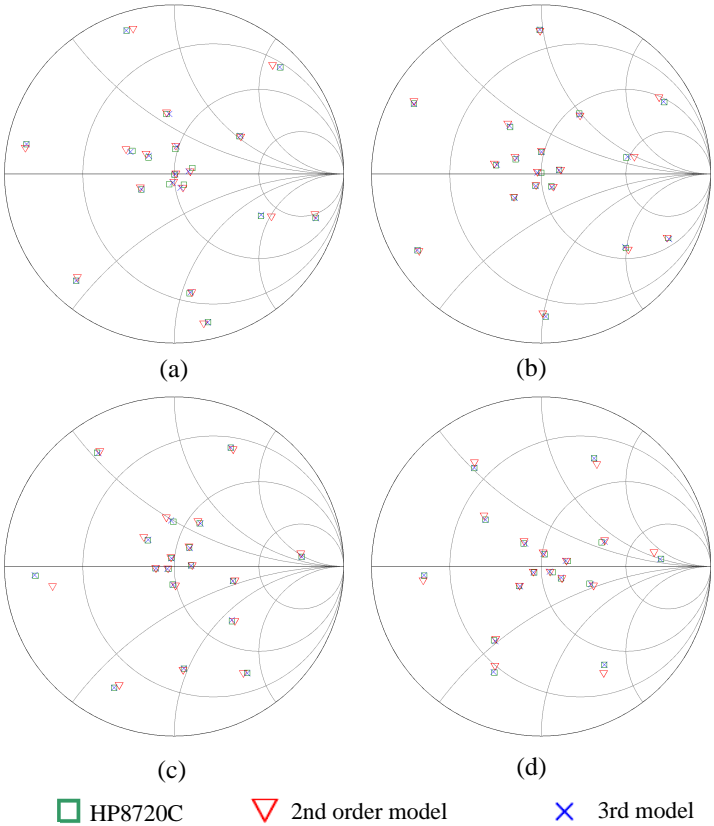


**Figure 5.** Comparison of reflection coefficients. (a)  $F = 1$  GHz. (b)  $F = 2.45$  GHz. (c)  $F = 5$  GHz. (d)  $F = 10$  GHz.

In the reflection coefficient configuration, the port 2 is connected to a matched load (Fig. 3) and a test load made of a sliding-short circuit is used to set multiple magnitudes  $|S_{11}|$  and phase-shifts  $\Phi_{11}$  of  $S_{11}$ . 18 loads are considered in this study. For each load, the reflection coefficient is retrieved from the detected voltages by the inversion procedure developed. The comparison observed between the measured data obtained by the four-port system and those provided by a HP8720C network analyzer are reported for four test frequencies in Fig. 5.

Theses graphs indicate that the third order model achieves a significantly better measurement accuracy than the second order model for the four test frequencies considered.

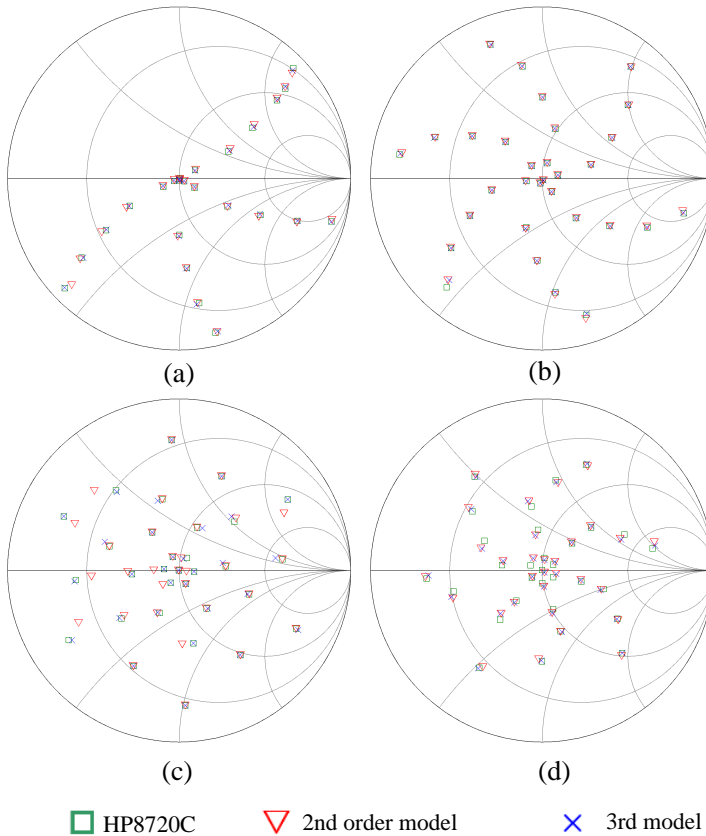


**Figure 6.** Comparison of transmission coefficients. (a)  $F = 1$  GHz. (b)  $F = 2.45$  GHz. (c)  $F = 5$  GHz (d).  $F = 10$  GHz.

In the following, we focus on the measurement of transmission coefficients in the frequency band 1–10 GHz. Thus, different loads made of a variable attenuator connected to a phase-shifter are measured with a HP8720C network analyzer and the proposed system. In Fig. 6, we present a comparison between these two kinds of data, for the same test of frequencies.

The conclusion drawn after the examination of these plots is that the results show relatively low deviations and confirm the performance of the third order model for all the frequencies considered. The system has been tested in the whole frequency band between 1 and 10 GHz with a step frequency of 1 GHz for both configurations, reflection and transmission. Equivalent measurement performance has been found. It has to be mentioned that the low differences between the findings obtained by the proposed system and the network analyzer HP8720C can be imputed to the mechanical reproducibility of the test loads.

To resume these experiments, we have demonstrated that an appropriate calibration technique can be applied to extend the frequency band capabilities (up to 10 GHz) of a microwave system that is initially designed and optimized to operate in a reduced frequency range (1–4 GHz). Thus, the microwave part of the system fabricated on the basis of a low-cost technology demonstrates the possibility to develop high performance network analysis tools at very low cost.

## 5. CONCLUSION

A new forward four-port network analyzer has been presented. The solution proposed eliminates the need of complex heterodyne principle and mechanical and bulky devices of the classical dual six-port network analyzer. The whole system is implemented on a single planar substrate and is well suited for monolithic integration. The fabricated system operates in the frequency band 1–10 GHz and comparisons with a conventional network analyzer have shown relatively low deviations. The system combines the attributes of low-cost, compactness, simplicity in realization and is well suited to address new applications where the traditional automatic network analyzer is generally oversized. In particular, a promising application field is microwave non destructive testing and evaluation.

## REFERENCES

1. Anderson, R. W., “*S*-parameter techniques for faster, more accurate network design,” *Hewlett-Packard Journal*, 1967.

2. Engen, G. F. and C. A. Hoer, "Application of an arbitrary six-port junction to power-measurement problems," *IEEE Trans. Instrum. Meas.*, Vol. 21, No. 4, 470–474, 1972.
3. Engen, G. F., "The six-port reflectometer. An alternative network analyzer," *IEEE Trans. Microw. Theory Tech.*, Vol. 25, No. 12, 1075–1080, 1977.
4. Cronson, H. M. and R. A. Fong-Tom, "A 94-GHz diode-based single six-port reflectometer," *IEEE Trans. Microw. Theory Tech.*, Vol. 30, No. 8, 1260–1264, 1982.
5. Ghannouchi, F. M. and R. G. Bosisio, "A comparative worst-case error analysis of some proposed six-port designs," *IEEE Trans. Instrum. Meas.*, Vol. 37, No. 4, 552–556, 1988.
6. Yeo, S. P. and K. H. Lee, "Improvements in design of six-port reflectometer comprising symmetrical five-port waveguide junction and directional coupler," *IEEE Trans. Instrum. Meas.*, Vol. 39, No. 1, 184–188, 1990.
7. Engen, G. F., "A (historical) review of the six-port measurement technique," *IEEE Trans. Microw. Theory Tech.*, Vol. 45, No. 12, 2414–2417, 1997.
8. Fang, X. T., X.-C. Zhang, and C.-M. Tong, "A novel miniaturized microstrip six-port junction," *Progress In Electromagnetics Research Letters*, Vol. 23, 129–135, 2011.
9. Haddadi, K., M. Wang, D. Glay, and T. Lasri, "A 60 GHz six-port distance measurement system with sub-millimeter accuracy," *IEEE Microw. Wireless Compon. Lett.*, Vol. 19, No. 10, 644–646, 2009.
10. Boukari, B., E. Moldovan, S. Affes, K. Wu, R. G. Bosisio, and S. O. Tatu, "A heterodyne six-port FMCW radar sensor architecture based on beat signal phase slope techniques," *Progress In Electromagnetics Research*, Vol. 93, 307–322, 2009.
11. Peng, H., Z. Yang, and T. Yang, "Calibration of a six-port receiver for direction finding using the artificial neural network technique," *Progress In Electromagnetics Research Letters*, Vol. 27, 17–24, 2011.
12. Peng, H., T. Yang, and Z. Yang, "Calibration of a six-port position sensor via support vector regression," *Progress In Electromagnetics Research C*, Vol. 26, 71–81, 2012.
13. Khaddaj Mallat, N., E. Moldovan, and S. O. Tatu, "Comparative demodulation results for six-port and conventional 60 GHz direct conversion receivers," *Progress In Electromagnetics Research*, Vol. 84, 437–449, 2008.

14. Khaddaj Mallat, N., E. Moldovan, and S. O. Tatu, "V-band quadrature phase shift keying demodulator using WR-12 six-port," *Progress In Electromagnetics Research Letters*, Vol. 6, 193–199, 2009.
15. Moscoso-Martir, A., I. Molina-Fernandez, and A. Ortega-Monux, "Signal constellation distortion and ber degradation due to hardware impairments in six-port receivers with analog I/Q generation," *Progress In Electromagnetics Research*, Vol. 121, 225–247, 2011.
16. De la Morena-Álvarez-Palencia, C. and M. Burgos-Garcia, "Four-octave six-port receiver and its calibration for broadband communications and software defined radios," *Progress In Electromagnetics Research*, Vol. 116, 1–21, 2011.
17. Hoer, C. A., "A network analyzer incorporating two six-port reflectometers," *IEEE Trans. Microw. Theory Tech.*, Vol. 25, 1070–1074, 1977.
18. Cronson, H. M. and L. Susman, "A dual six-port network analyzer," *IEEE Trans. Microw. Theory Tech.*, Vol. 29, No. 4, 372–378, 1981.
19. Moyer, R. D., "An inexpensive implementation of a dual six-port 0.01- to 18-GHz network analyzer," *IEEE Trans. Instrum. Meas.*, Vol. 32, No. 1, 279–285, 1983.
20. Judah, S. R. and A. S. Wright, "A dual six-port network analyzer incorporating a biphas-bimodulation element," *IEEE Trans. Microw. Theory Tech.*, Vol. 38, No. 3, 238–244, 1990.
21. Haddadi, K., M. Wang, D. Glay, and T. Lasri, "Ultra wide-band four-port reflectometer using only two quadratic detectors," *Proceedings of the IEEE MTT-S Symposium*, 379–382, Atlanta, USA, 2008.
22. Haddadi, K. and T. Lasri, "Formulation for complete and accurate calibration of six-port reflectometer," *IEEE Trans. Microw. Theory Tech.*, Vol. 60, No. 3, 574–581, 2012.
23. Haddadi, K., M. Wang, K. Nouri, D. Glay, and T. Lasri, "Calibration and performance of two new ultra wide-band four-port based systems," *IEEE Trans. Microwave Theory Tech.*, Vol. 56, No. 12, 3137–3142, 2008.
24. Haddadi, K., M. Wang, D. Glay, and T. Lasri, "A new range finder based on a four-port junction," *IEEE Sensors Journal*, Vol. 9, No. 6, 697–698, 2009.
25. Wang, M., K. Haddadi, D. Glay, and T. Lasri, "Compact near-field microwave microscope based on the multi-port technique,"

- Proceedings of the 2010 European Microwave Conference (EuMC)*, 771–774, Paris, France, 2010.
26. Haddadi, K., H. El Aabbaoui, C. Loyez, D. Glay, N. Rolland, and T. Lasri, “Wide-band 0.9 GHz to 4 GHz four-port receiver,” *Proceedings of the IEEE Int. Conf. Electron. Circuits and Systems*, 1316–1319, Nice, France, 2006.
  27. Haddadi, K., M. M. Wang, C. Loyez, D. Glay, and T. Lasri, “Four-port communication receiver with digital IQ-regeneration,” *IEEE Microw. Wireless Compon. Lett.*, Vol. 20, No. 1, 58–60, 2010.